Acta Cryst. (1999). B**55**, 24–30

High-temperature phases of $NaNbO_3$ and $NaTaO_3$

C. N. W. Darlington[a]* and K. S. Knight[b]

[a]*School of Physics and Astronomy, University of Birmingham, Birmingham B15 2TT, England, and* [b]*Rutherford Appleton Laboratory, Chilton, Didcot OX11 0QX, England. E-mail: c.n.w.darlington@bham.ac.uk*

(*Received 13 November 1997; accepted 14 July 1998*)

Abstract

The high-temperature phases of the perovskites sodium niobate, $NaNbO_3$, and sodium tantalate, $NaTaO_3$, have been re-examined using the high-resolution powder diffractometer HRPD at the ISIS neutron spallation source; the two materials show the same sequence of phases with tilted octahedra. Diffraction patterns were measured every 5 K allowing structural changes with temperature within a single phase to be determined for the first time. Previous structure determinations within one phase had been performed at a single temperature only. The octahedra are tilted about pseudocubic ⟨100⟩ directions and are also deformed; the magnitude of the deformation is shown to be proportional to the square of the angle of tilt as expected from a phenomenological theory applied to such transitions. The structures of $NaNbO_3$ between 753 and 793 K and of $NaTaO_3$ below 758 K are not as reported in the literature.

1. Introduction

Both sodium niobate and sodium tantalate undergo a sequence of displacive phase transitions involving octahedral rotations or tilts at high temperatures. The tilt systems proposed in the literature involve rotation of the octahedra about axes which are parallel to ⟨100⟩ pseudocubic directions. Along the axes of rotation the tilts are either in the same or in opposite senses. The tilts double the pseudocubic repeat distances in directions perpendicular to the rotation axes, while the repeat distance along the rotation axis remains approximately the same if the tilts are in the same sense or doubled if in opposite senses.

Glazer (1972) introduced a convenient notation to describe the most commonly found tilt systems: tilts with the same sense along the rotation axis are allocated a plus sign, those with opposite senses a minus sign. If the magnitude of the tilt angles about ⟨100⟩ pseudocubic directions are the same, then they are given the same letter, if not a different letter is used. So the tilt system with three equal tilts with opposite senses along the rotation axes is described as $[a^-a^-a^-]$; three unequal tilts of the same sense as $[a^+b^+c^+]$. The cubic phase is given the symbol $[a^0a^0a^0]$.

The transitions are displacive and the small atomic displacements present in the low-symmetry phases can be described in terms of condensed normal modes of the cubic phase (Cochran & Zia, 1968). A plus tilt has a wavevector of $(0, \frac{1}{2}, \frac{1}{2})$ and symmetry-related positions (the *M* points of the cubic Brillouin zone) while a minus tilt has wavevector $(\frac{1}{2}, \frac{1}{2}, \frac{1}{2})$, the *R* point. We will use the notation M_i to describe the magnitude of a plus tilt about the *i*th pseudocubic ⟨100⟩ direction and R_i the magnitude of a minus tilt.

The high-temperature structures reported in the literature for $NaNbO_3$ (Glazer & Megaw, 1972; Ahtee *et al.*, 1972; Ishida & Honjo, 1972) and for $NaTaO_3$ (Ahtee & Unonius, 1977; Ahtee & Darlington, 1980) are given in Table 1. Rietveld structural refinements have been carried out for all three low-symmetry phases of sodium tantalate and for phase T_1 of sodium niobate (Ahtee & Darlington, 1980), but only at a single temperature within each phase.

We have re-examined all the phases listed in Table 1 in both materials using the high-resolution powder diffractometer HRPD on the neutron spallation source at the Rutherford Appleton Laboratory. Rietveld refinements of these structures have been performed at 5 K intervals allowing structural changes with temperature within a single phase to be evaluated for the first time. Both structures with three tilts – phase S of $NaNbO_3$ between 753 and 793 K, and $NaTaO_3$ below 758 K – are different from those described in the literature (and different from each other). Work is continuing on the refinement of these two structures and will be the subject of separate papers. However, the structures above 793 K ($NaNbO_3$) and above 758 K ($NaTaO_3$) refined successfully with the tilt systems and space groups given in Table 1.

The paper is in the following format: the refinement procedure is briefly described in §2, in §3 the temperature dependence of the magnitudes of the rotation angles and other relevant structural parameters are discussed and in §4 the 'observed' and 'calculated' macrostrains are compared. In §5, the deformation of the octahedra is discussed.

2. Data collection, reduction and refinement

Powders of the two materials were purchased from Alfa, a Johnson Matthey company. Sodium niobate was 99.997% pure on a metals basis, while sodium tantalate

ISSN 0108-7681

Table 1. *High-temperature structures of $NaNbO_3$ and $NaTaO_3$ reported in the literature*

$NaNbO_3$[(a)]	753 K [$a^+b^-c^+$]	793 K [$a^0b^-c^+$]	848 K [$a^0b^0c^+$]	914 K [$a^0b^0c^0$]
	[M_1 R_2 M_3]	[0 R_2 M_3]	[0 0 M_3]	[0 0 0]
Space group	*Pmnm*	*Cmcm*	*P*4/*mbm*	$Pm\bar{3}m$
Phase label	S	T_1	T_2	U
$NaTaO_3$[(b)]	0 K [$a^-a^-c^+$]	758 K [$a^0b^-c^+$]	838 K [$a^0b^0c^+$]	903 K [$a^0a^0a^0$]
	[$R_1 = R_2$ M_3]	[0 R_2 M_3]	[0 0 M_3]	[0 0 0]
Space group	*Pnam*	*Cmcm*	*P*4/*mbm*	$Pm\bar{3}m$

References: (*a*) Glazer & Megaw (1972); Ahtee *et al.* (1972); Ishida & Honjo (1972); (*b*) Ahtee & Darlington (1980).

was 99.9+% pure. The average particle diameter was about 5 μm.

Neutron powder diffraction patterns were collected using the high-resolution powder diffractometer HRPD (Ibberson *et al.*, 1992) at the ISIS spallation source using the lower resolution 1 m position. Approximately 3 cm^3 of powder were contained in a thin-walled vanadium sample can with an internal diameter of 11 mm. The can was connected to the centre stick of a standard ISIS furnace and the whole furnace was evacuated to 5×10^{-4} mbar (1 bar = 10^5 Pa). The sample temperature was measured using a chromel/alumel thermocouple mounted on the surface of the can approximately 2 cm from the centre of the neutron beam. During all runs the temperature variation was less than ±2 K. Data were collected in time-of-flight mode using logarithmic time-channel binning of $\Delta t/t = 1 \times 10^{-4}$, from 32 to 122 ms, which corresponds to a measured *d*-spacing range of 0.65 to 2.5 Å for the back-scattering detectors. The resolution of the instrument, full width at half maximum intensity, was $\Delta d/d = 8 \times 10^{-4}$ over the whole diffraction pattern.

The raw data from the detector banks were focused to a common scattering angle of 163.329°, normalized to an upstream monitor and corrected for detector efficiency using a vanadium standard. Finally, the data were corrected for wavelength-dependent absorption in the vanadium tails of the furnace and rebinned in $\Delta t/t = 3 \times 10^{-4}$, which gave the required resolution for the sample.

Initial data analysis was carried out using structural-model-independent fits (Pawley, 1981) for each temperature using the modified time-of-flight Rietveld program *TF*12*LS* (David *et al.*, 1992). Finally, full Rietveld analysis was carried out at each temperature.

3. Results and discussion

The phase with tilt system [0 R_2 M_3] or [$a^0b^-c^+$] has space group *Cmcm* (No. 63). Atomic coordinates are given in Table 2.† The unit cell is in parallel orientation: the directions of the orthorhombic lattice vectors are in the same directions as the original ⟨100⟩ cubic vectors. The magnitudes of the orthorhombic lattice parameters are approximately twice those of the cubic phase. Tilt system [0 0 M_3] or [$a^0a^0c^+$] has space group *P*4/*mbm* (No. 127) and the atomic positions are listed in Table 3. The tetragonal lattice parameters have approximate magnitudes [$2^{1/2}$ $2^{1/2}$ 1] times those of the cubic parameter. The cubic phase has space group $Pm\bar{3}m$ (No. 221).

Listed in Tables 2 and 3 are the relationships between the tilt angles and the atomic displacements. The cations showed nearly isotropic vibrational amplitudes, while the O atoms showed significant anisotropy with much larger vibrational amplitudes in directions perpendicular to the Nb—O and Ta—O bonds than along these bonds. In all the refinements reported here, isotropic displacement factors were used for Na, Nb and Ta atoms, and anisotropic parameters for the O atoms. This significantly reduced the number of parameters required in the refinement. For a particular temperature in each phase the atomic parameters and displacement factors are given in Tables 2 and 3.

Figs. 1 and 2 show the temperature dependence of the pseudocubic lattice parameters of the two materials. The temperature variation of the macrostrains will be discussed in greater detail in §4. Note that the transitions in both materials appear to be continuous; they are allowed to be so from Landau theory.

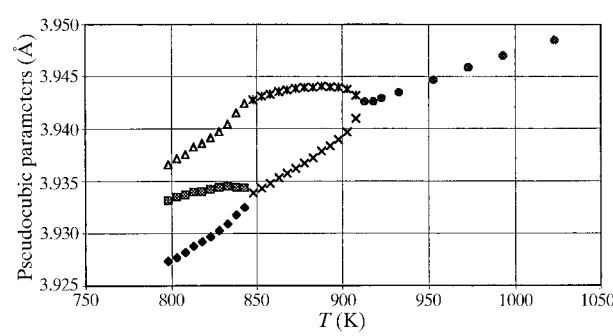

Fig. 1. The temperature dependence of the pseudocubic (pc) lattice parameters in $NaNbO_3$. Filled diamonds: a_{pc}; cross-hatched squares: b_{pc}; triangles: c_{pc}; crosses: $a_{pc} = b_{pc}$; asterisks: c_{pc}; circles: *a*(cubic).

† Supplementary data for this paper are available from the IUCr electronic archives (Reference: BM0015). Services for accessing these data are described at the back of the journal.

Table 2. *Atomic coordinates for phase [0 R_2 M_3] ≡ [0b^-c^+], space group Cmcm, No. 63*

	x	y	z
Nb/Ta	1/4	1/4	0
Na1	0	y_{A1}	1/4
Na2	0	1/2 + y_{A2}	1/4
O1	1/4 + x_{O1}	0	0
O2	0	1/4 + y_{O2}	z_{O2}
O3	1/4 + x_{O3}	1/4 + y_{O3}	1/4

$$\tan(R_2) = 4z_{O2}(c_{pc}/a_{pc})$$
$$\tan(R_2) = 4x_{O3}(a_{pc}/c_{pc})$$
$$\tan(M_3) = 4x_{O1}(a_{pc}/b_{pc})$$
$$\tan(M_3) = 4y_{O2}(b_{pc}/a_{pc})$$

Atomic parameters for $NaNbO_3$ at 813 K. B values are given in Å^2.

Nb	B_{iso} = 1.60 (1)		
Na1(y_{A1}) = 0.0022 (14)	B_{iso} = 3.56 (12)		
Na2(y_{A2}) = 0.0026 (14)	B_{iso} = 4.31 (14)		
O1(x_{O1}) = −0.0270 (4)			
B^{11} = 3.12 (12)	B^{22} = 0.77 (8)	B^{33} = 5.41 (21)	B^{23} = 0.07 (13)
O2(y_{O2}) = 0.0241 (4)	O2(z_{O2}) = 0.0203 (3)		
B^{11} = 1.49 (6)	B^{22} = 3.75 (14)	B^{33} = 3.33 (15)	B^{23} = −0.16 (10)
O3(x_{O3}) = 0.0210 (3)	O3(y_{O3}) = −0.0011 (7)		
B^{11} = 3.31 (13)	B^{22} = 4.60 (16)	B^{33} = 1.42 (7)	B^{12} = 0.65 (16)

Atomic parameters for $NaTaO_3$ at 803 K. B values are given in Å^2.

Ta	B_{iso} = 0.98 (2)		
Na1(y_{A1}) = 0.0077 (21)	B_{iso} = 3.29 (20)		
Na2(y_{A2}) = 0.0074 (21)	B_{iso} = 3.37 (20)		
O1(x_{O1}) = −0.0247 (5)			
B^{11} = 2.31 (17)	B^{22} = 0.36 (12)	B^{33} = 4.70 (29)	B^{23} = 0.14 (25)
O2(y_{O2}) = 0.0239 (6)	O2(z_{O2}) = 0.0200 (5)		
B^{11} = 1.24 (9)	B^{22} = 3.00 (20)	B^{33} = 3.27 (24)	B^{23} = −1.04 (16)
O3(x_{O3}) = 0.0237 (5)	O3(y_{O3}) = −0.0022 (11)		
B^{11} = 3.49 (18)	B^{22} = 3.10 (21)	B^{33} = 1.23 (11)	B^{12} = 0.77 (25)

Figs. 3 and 4 give the temperature variation of the magnitude of the M_3 and R_2 tilts in $NaNbO_3$; Figs. 5 and 6 show the tilts in $NaTaO_3$.

Several comments are worth recording:

(i) The quality of the Rietveld fits was better for $NaNbO_3$ than for $NaTaO_3$. The standard uncertainties of the displacements for $NaTaO_3$ were typically 50% larger than those of $NaNbO_3$. No impurity peaks were detected in the pattern for $NaNbO_3$. However, we detected the presence of $Na_2Ta_4O_{11}$ (Ercit *et al.*, 1985) *via* extremely weak peaks in the pattern for $NaTaO_3$ which would account for the slightly less satisfactory refinements for the tantalate.

(ii) The tilt angles calculated from the actual atomic displacements are considerably bigger, by about a factor of two, than those estimated from lattice parameters and the assumption that the octahedra are regular. For example, Ahtee *et al.* (1972) give the

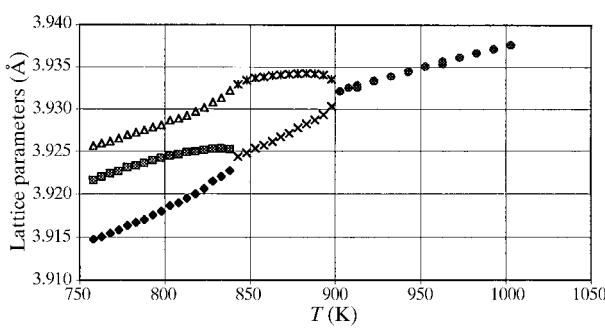

Fig. 2. The temperature dependence of the pseudocubic (pc) lattice parameters in $NaTaO_3$. Filled diamonds: a_{pc}; cross-hatched squares: b_{pc}; triangles: c_{pc}; crosses: $a_{pc} = b_{pc}$; asterisks: c_{pc}; circles: a(cubic).

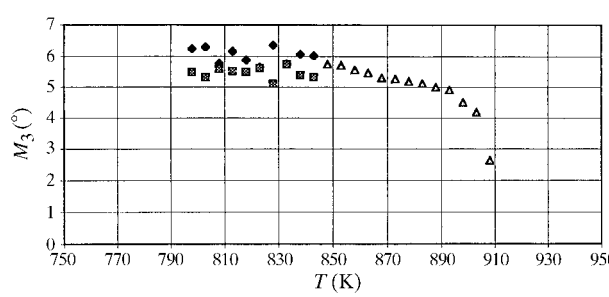

Fig. 3. The temperature dependence of the magnitude of the plus tilts in $NaNbO_3$. Filled diamonds represent values calculated from the displacements of O1(x) and cross-hatched squares represent values calculated from the displacements of O2(y).

Table 3. *Atomic coordinates for phase [0 0 M_3] ≡ [00c$^+$], space group P4/mbm, No. 127*

	x	y	z
Nb/Ta	0	0	0
Na	0	1/2	1/2
O1	0	0	1/2
O2	$1/4 + x_{O2}$	$1/4 - x_{O2}$	0

$$\tan(M_3) = 4x_{O2}$$

Atomic parameters for $NaNbO_3$ at 888 K. B values are given in Å^2.

Nb	$B_{iso} = 1.64$ (1)	
Na	$B_{iso} = 4.26$ (3)	
O1	$B^{11} = B^{22} = 5.02$ (7)	$B^{33} = 1.29$ (5)
O2(x_{O2}) = 0.0219 (1)		
$B^{11} = B^{22} = 2.45$ (3)	$B^{33} = 5.15$ (5)	$B^{12} = -1.22$ (4)

Atomic parameters for $NaTaO_3$ at 878 K. B values are given in Å^2.

Ta	$B_{iso} = 1.05$ (2)	
Na	$B_{iso} = 3.75$ (4)	
O1	$B^{11} = B^{22} = 4.41$ (11)	$B^{33} = 1.11$ (8)
O2(x_{O2}) = 0.0213 (2)		
$B^{11} = B^{22} = 2.07$ (5)	$B^{33} = 4.53$ (8)	$B^{12} = -1.22$ (6)

magnitude of M_3 for $NaNbO_3$ at 823 K as 3.5° compared with our value of around 6°. The reason for this discrepancy is the considerable deformation of the octahedron (see §5).

(iii) The magnitude of the M_3 tilt decreases quite rapidly as the transition to the cubic phase is approached from below. This indicates that the critical exponent β is less than 0.5, the mean-field value (see the discussion in §4).

(iv) In $NaNbO_3$ the magnitudes of the M_3 tilt deduced from O1(x) and from O2(y) in phase T_1 are extremely close in value. The same is true for the R_2 tilt deduced from O3(x) and O2(z) in $NaNbO_3$. In $NaTaO_3$, although the magnitudes of the M_3 tilts over the whole temperature range are in good agreement, the R_2 tilts are not. In particular the R_2 tilt deduced from O3(x) shows very little temperature dependence. Why this should be the case we do not know.

(v) In both materials the magnitude of the M_3 tilt is not affected by the disappearance of the R_2 tilt.

In the phase with two tilts, [0 R_2 M_3], additional displacements are allowed other than those associated with pure octahedral rotations. The displacements are Na1(y), Na2(y) and O3(y). It was pointed out (Fujii *et al.*, 1974; Hirotsu *et al.*, 1974) that in phase T_2, [0 R_2 M_3], since the M point, $(\frac{1}{2}, \frac{1}{2}, 0)$, of the original cubic phase has become a Γ point, the X and R points, $(0, 0, \frac{1}{2})$ and $(\frac{1}{2}, \frac{1}{2}, \frac{1}{2})$, respectively, are connected by a reciprocal lattice vector and hence are equivalent points. Consequently, the modes at the R point can no longer be purely rotational modes. It was argued (Darlington, 1976) that the additional displacements should be describable in terms of normal modes of the cubic phase with the wavevector of the relevant X point, which is $(0, 0, \frac{1}{2})$.

Cowley (1964) has listed the normal modes for the cubic phase and from this one finds that the relevant mode with wavevector $(0, 0, \frac{1}{2})$ is doubly degenerate, transverse, and transforms like irreducible representation M_5'. The allowed displacement of the atoms in the

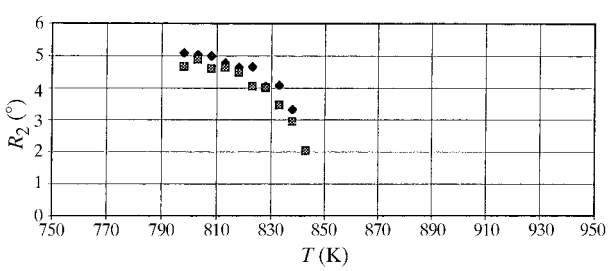

Fig. 4. The temperature dependence of the magnitude of the minus tilts in $NaNbO_3$. Filled diamonds represent values calculated from the displacements of O3(x) and cross-hatched squares represent values calculated from the displacements of O2(x).

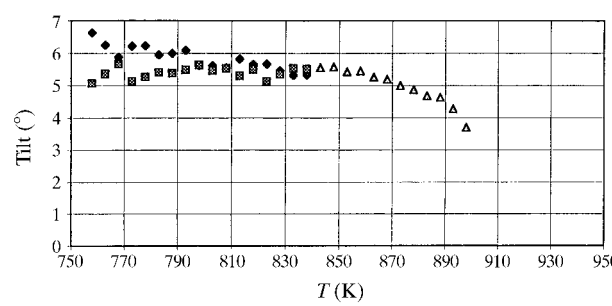

Fig. 5. The temperature dependence of the magnitude of the plus tilts in $NaTaO_3$. Filled diamonds represent values calculated from the displacements of O1(x) and cross-hatched squares represent values calculated from the displacements of O2(y).

cubic phase are [Na(x), O3(x)] and [Na(y), O3(y)] and have a staggered sequence along [001].

In the phase with space group *Cmcm* only one component, the y component, of the doubly degenerate mode has condensed out. The space group *Cmcm* allows different magnitudes and signs for the displacement of Na1(y) and Na2(y), but if the displacements are to be like those of the y component of the X mode [$(0, 0, \frac{1}{2})$, M_5'] of the cubic phase, then these displacements must have the same sign and magnitude. From Table 2 it is seen that within the estimated error this is the case. The same is true for many perovskites (Ahtee & Darlington, 1980). Thus the number of parameters needed to describe this structure is actually less than the number of independent parameters allowed by the space group.

4. Macrostrains

The pseudocubic lattice parameters are related to the macrostrains, ε_{ij}, by

$$a_i = a_{c0}(1 + \gamma T + \varepsilon_{ii})$$

and

$$\alpha_i = \pi/2 - 2\varepsilon_{jk}$$

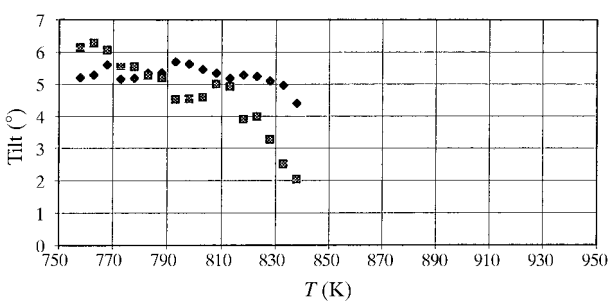

Fig. 6. The temperature dependence of the magnitude of the minus tilts in $NaTaO_3$. Filled diamonds represent values calculated from the displacements of O3(x) and cross-hatched squares represent values calculated from the displacements of O2(z).

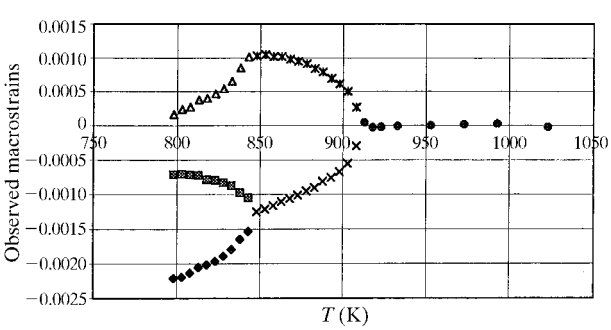

Fig. 7. The temperature dependence of the macrostrains obtained by subtracting the effects of thermal expansion from the measured pseudocubic lattice parameters of $NaNbO_3$. Filled diamonds: ε_{11}; cross-hatched squares: ε_{22}; triangles: ε_{33}; crosses: $\varepsilon_{11} = \varepsilon_{22}$; asterisks: ε_{33}; circles: $\varepsilon_{11} = \varepsilon_{22} = \varepsilon_{33}$.

where a_{c0} is the value of the cubic lattice parameter extrapolated to absolute zero, γ is the thermal expansion coefficient (assumed to be independent of temperature), and T is the temperature. Values for a_{c0} and γ were obtained by fitting a straight line to the temperature dependence of the cubic lattice parameter; values for the macrostrains could then be obtained and these are shown in Figs. 7 and 8 for $NaNbO_3$ and $NaTaO_3$, respectively.

From a Landau expansion in terms of the magnitudes of the angles of rotation, R_i and M_i, the macrostrains ε_{ij} and coupling terms (Darlington, 1996), it was shown that to first order the macrostrains are related to the square of the angles of rotation in much the same way that the macrostrain in a ferroelectric is related to the square of the spontaneous polarization. We have

$$\varepsilon_{ii} = S_{11}R_i^2 + S_{12}(R_j^2 + R_k^2) + T_{11}M_i^2 + T_{12}(M_j^2 + M_k^2)$$
$$\varepsilon_{ij} = S_{44}R_iR_j + U_{44}X_k^{(i)}X_k^{(j)} \qquad (1)$$

where the coefficients S_{ij}, T_{ij} and U_{44} are taken to be sensibly temperature independent. $X_k^{(i)}$ is proportional to the magnitude of the condensed mode with wavevector $(0, 0, \frac{1}{2})$ as discussed in §3. For example, $X_3^{(2)}$ describes the displacements of Na1, Na2 and O3 in the y direction with wavevector $(0, 0, \frac{1}{2})$.

If the octahedra were to remain undistorted when tilted, then the coefficients S_{ij} and T_{ij} would have definite values, namely

$$S_{11} = T_{11} = 0$$
$$S_{12} = T_{12} = -1/2$$
$$S_{44} = 1/2$$

if the magnitudes of the tilts are expressed in radians.

Substituting the non-zero octahedral tilts into (1) leads to the following expressions for the macrostrains in the two phases:

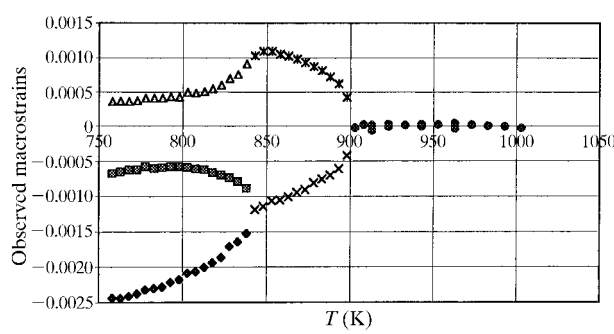

Fig. 8. The temperature dependence of the macrostrains obtained by subtracting the effects of thermal expansion from the measured pseudocubic lattice parameters of $NaTaO_3$. Filled diamonds: ε_{11}; cross-hatched squares: ε_{22}; triangles: ε_{33}; crosses: $\varepsilon_{11} = \varepsilon_{22}$; asterisks: ε_{33}; circles: $\varepsilon_{11} = \varepsilon_{22} = \varepsilon_{33}$.

$$\text{phase } T_1, [0\ R_2\ M_3]\quad \begin{aligned}\varepsilon_{11} &= S_{12}R_2^2 + T_{12}M_3^2\\ \varepsilon_{22} &= S_{11}R_2^2 + T_{12}M_3^2\\ \varepsilon_{33} &= S_{12}R_2^2 + T_{11}M_3^2\\ \varepsilon_{23} &= \varepsilon_{31} = \varepsilon_{12} = 0\end{aligned} \qquad (2)$$

$$\text{phase } T_2, [0\ 0\ M_3]\quad \begin{aligned}\varepsilon_{11} &= \varepsilon_{22} = T_{12}M_3^2\\ \varepsilon_{33} &= T_{11}M_3^2\\ \varepsilon_{23} &= \varepsilon_{31} = \varepsilon_{12} = 0.\end{aligned} \qquad (3)$$

Calculated macrostrains were obtained from relationships (2) and (3) and the experimentally determined tilt angles shown in Figs. 3–6. Values used for M_3 in phase T_1 were those calculated from the displacement of O1(x), for both $NaNbO_3$ and $NaTaO_3$. Values for R_2 were obtained from O3(x) for $NaNbO_3$ and from O2(z) for $NaTaO_3$. Calculated macrostrains, shown in Figs. 9 and 10, use values for S_{ij} and T_{ij} given in Table 4; these values gave the 'best fit' to the observed macrostrains. (The magnitudes of the angles were expressed in radians.)

The greater scatter of points in the two phases with tilts [0 R_2 M_3] compared to those in phases with tilt [0 0 M_3] is a consequence of the greater scatter of points describing the octahedral rotation in Figs. 3—6. This is a consequence of the number of independent structural parameters increasing from eight for [0 0 M_3] to 22 for [0 R_2 M_3].

The agreement is quite good over the whole temperature range. Therefore S_{ij} and T_{ij} are not only independent of temperature, but have the same values in each phase; they have the same standing as the electrostrictive constants that relate macrostrain to the square of the spontaneous polarization.

If mean-field theory were to apply, then the square of the angle would vary linearly with temperature and the calculated macrostrains in Figs. 9 and 10 would be a series of straight lines. The curvature indicates that either the magnitude of the rotation saturates, or, more probably, that the critical exponent β is less than 0.5.

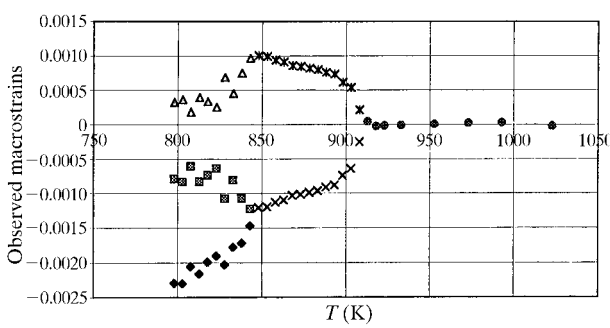

Fig. 9. The temperature dependence of the macrostrains obtained from the magnitudes of the octahedral rotations determined from structural refinements and the values of S_{ij} and T_{ij} given in Table 4 for $NaNbO_3$.

Table 4. *Magnitudes of parameters used to calculate the macrostrain (tilt angles in radians)*

	a_{c0} (Å)	γ (K^{-1})	S_{11}	S_{12}	T_{11}	T_{12}
$NaNbO_3$	3.89010	1.44705×10^{-5}	0.08	−0.11	0.10	−0.12
$NaTaO_3$	3.88246	1.42003×10^{-5}	0.08	−0.10	0.12	−0.12

5. Octahedral deformation

The values of the coefficients S_{ij} and T_{ij} are very different from those expected for regular, undeformed octahedra. Examination of the literature shows that in all perovskites for which accurate lattice parameters have been reported, S_{11} and T_{11} are positive rather than zero, and S_{12} and T_{12} are negative but significantly greater than $-\frac{1}{2}$. S_{44} and U_{44} can only be evaluated from the temperature dependence of the interaxial angle in phases with two or more minus tilts, and therefore cannot be determined from the phases of $NaNbO_3$ and $NaTaO_3$ discussed here. For those phases with two or more minus tilts, S_{44} is found to be negative rather than $+\frac{1}{2}$ (Darlington, 1996).

Changes in the shape of the octahedron cannot be determined from the values of S_{ij} and T_{ij} alone, since the octahedra are tilted. The octahedra in the phases

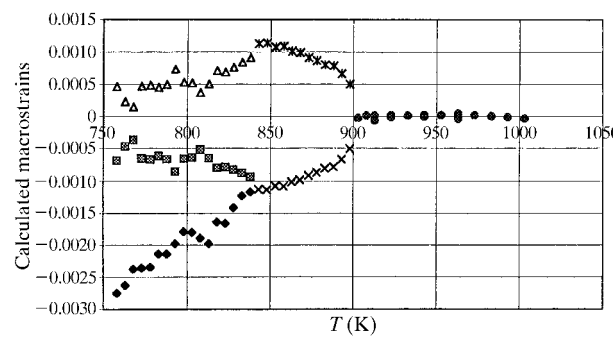

Fig. 10. The temperature dependence of the macrostrains obtained from the magnitudes of the octahedral rotations determined from structural refinements and the values of S_{ij} and T_{ij} given in Table 4 for $NaTaO_3$.

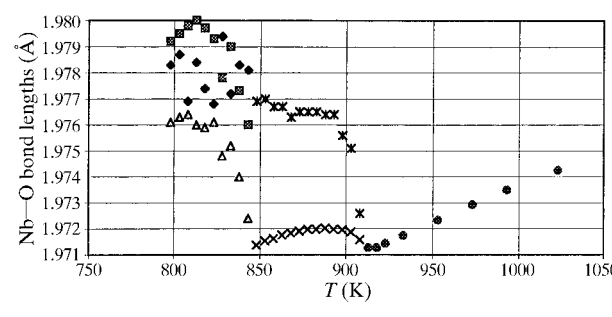

Fig. 11. The temperature dependence of the Nb—O bond lengths in $NaNbO_3$. Phase *Cmcm*: filled diamonds represent Nb—O1, cross-hatched squares represent Nb—O2 and triangles represent Nb—O3. Phase *P*4/*mbm*: crosses represent Nb—O1, asterisks represent Nb—O2. Phase $m\bar{3}m$: circles represent Nb—O.

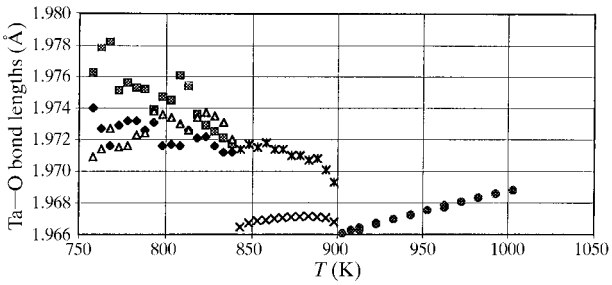

Fig. 12. The temperature dependence of the Ta—O bond lengths in $NaTaO_3$. Phase *Cmcm*: filled diamonds represent Ta—O1, cross-hatched squares represent Ta—O2, triangles represent Ta—O3. Phase *P*4/*mbm*: crosses represent Ta—O1, asterisks represent Ta—O2. Phase $m\bar{3}m$: circles represent Ta—O.

examined here are centrosymmetric and the pseudo-cubic axes are orthogonal, hence the Nb—O/Ta—O bond lengths give information on octahedral deformation. These are shown in Figs. 11 and 12 for $NaNbO_3$ and $NaTaO_3$, respectively. These figures depict the measured bond lengths and have not had the effects of thermal expansion removed.

On entering the phase with a single plus tilt from the cubic phase, there is a relaxation of the bond length perpendicular to the rotation axis – about four times that of the expansion along the rotation axis described by T_{11}. The combination of the tilt with relaxation of the bond length still leads to a negative macrostrain; T_{12} is negative but greater than $-\frac{1}{2}$, the value expected for regular octahedra. A similar relaxation of the bond length occurs at the transition from $[0\,0\,M_3]$ to $[0\,R_2\,M_3]$. To a reasonable approximation, from examination of Figs. 11 and 12, the relaxation is proportional to the magnitude of the tilts; the bonds lengthen by about 0.001 Å per degree of tilt.

6. Conclusions

The structures of the two highest-temperature phases of $NaNbO_3$ and $NaTaO_3$ have been determined at intervals of 5 K. The evolution of these structures with temperature has been determined for the first time and is well described by a phenomenological theory based on a Landau expansion involving terms proportional to the tilt angles, strain, and terms coupling the tilt and strain. The octahedra become considerably deformed, with their deformation proportional to the squares of the angles of tilt. The structures reported in the literature for phase S ($NaNbO_3$) and for $NaTaO_3$ below 758 K are incorrect, and will be the subject of a different paper.

References

Ahtee, M. & Darlington, C. N. W. (1980). *Acta Cryst.* B**36**, 1007–1014.
Ahtee, M., Glazer, A. M. & Megaw, H. D. (1972). *Phil. Mag.* **26**, 995–1014.
Ahtee, M. & Unonius, L. (1977). *Acta Cryst.* A**33**, 150–154.
Cochran, W. & Zia, A. (1968). *Phys. Status Solidi*, **25**, 273–283.
Cowley, R. A. (1964). *Phys. Rev. A*, **134**, 981–997.
Darlington, C. N. W. (1976). *Phys. Status Solidi*, **76**, 231–239.
Darlington, C. N. W. (1996). *Phys. Status Solidi A*, **155**, 31–42.
David, W. I. F., Ibberson, R. M. & Matthewman, J. C. (1992). *Profile Analysis of Neutron Powder Diffraction Data at ISIS*. Report RAL-92-032. Rutherford Appleton Laboratory, Chilton, Didcot, England.
Ercit, T., Hawthorne, F. & Cerny, P. (1985). *Bull. Mineral.* **108**, 541–542.
Fujii, Y., Hoshino, S., Yamada, Y. & Shirane, G. (1974). *Phys. Rev. B*, **9**, 4549–4559.
Glazer, A. M. (1972). *Acta Cryst.* B**28**, 3384–3392.
Glazer, A. M. & Megaw, H. D. (1972). *Phil. Mag.* **25**, 1119–1135.
Hirotsu, S., Harada, J., Iizumi, M. & Gesi, K. (1974). *J. Phys. Soc. Jpn*, **37**, 1393–1398.
Ibberson, R. M., David, W. I. F. & Knight, K. S. (1992). *The High-Resolution Powder Diffractometer (HRPD) at ISIS – a User Guide.* Report RAL-92-031. Rutherford Appleton Laboratory, Chilton, Didcot, England.
Ishida, K. & Honjo, G. (1972). *J. Phys. Soc. Jpn*, **34**, 1279–1288.
Pawley, G. S. (1981). *J. Appl. Cryst.* **14**, 357–361.